Heritage Science

RESEARCH

Open Access

Effects of natural weathering on aged wood from historic wooden building: diagnosis of the oxidative degradation

Xiaochen Mi[1*], Yingqi Li[2], Xiaochao Qin[3] and Jie Li[4]

Abstract

Historic wooden buildings located outdoors are exposed to natural weathering conditions for extended periods of time, causing deterioration of wood properties by sunlight, oxygen, and other environmental factors. Current diagnostic procedures are limited to macroscopic inspection. In this interdisciplinary study, several aged samples from Yingxian Wooden Pagoda (ca. 1056 AD) were analyzed. Their micro-morphology and changes in chemical composition were investigated using less invasive multi-chemical techniques. The aim is to elucidate the oxidative degradation and its deterioration mechanism of the wood, which is essential in identifying the key factors responsible for natural weathering and devising strategies to counteract the surface deterioration. All aged wood samples had varying degrees of decay and lignin content was decreased in most of them. The high ratio of oxygen/carbon elements evidenced the occurrence of chemical reactions. In particular, the increasing ratio of oxygenated carbon/unoxygenated carbon indicates potential oxidation reactions. Overall, for the aged wood of historic wood building under warm-dry natural conditions, their deterioration occurred through the oxidative degradation of lignin. These unique results are useful in developing effective repair and restoration measures to conserve wooden components in historic buildings.

Keywords Historic wooden building, Aged wood, Oxidative degradation, Natural weathering, Chemical analysis

Introduction

Historic wooden buildings have recognized cultural, historical, and artistic values, reflecting the human productivity, technological skills, habit, and culture since the ancient times. However, such architectures under warm-dry natural conditions inevitably suffer damage from sunlight, oxygen, and other weathering factors. Compared to damage to the physical and mechanical properties of wood, surface decay is the most observed pattern of deterioration. This continuous decay process reduces the effective bearing section and bearing capacities of wooden components, jeopardizing the building survival. To effectively preserve and restore these buildings, it is important to find ways to diagnose the surface deterioration of aged wood components and understand the underlying deterioration mechanism.

Several scholars have extensively studied the structural seismic performance of historic buildings, such as their overall structure [1, 2] and their partial components (e.g., beam–column joints) [3, 4]. Besides, a wide range of wood properties have been investigated [5]. However, those studies focused on the macroscopic mechanical properties, while the chemical and morphological decay

*Correspondence:
Xiaochen Mi
mixiaochen1234@163.com
[1] School of Design and Art, Taiyuan University of Science and Technology, Taiyuan 030024, People's Republic of China
[2] College of Civil Engineering, Taiyuan University of Technology, Taiyuan 030024, People's Republic of China
[3] Shanxi Traffic Planning Survey and Design Institute Co., LTD, Taiyuan 030024, People's Republic of China
[4] School of Vehicle and Transportation Engineering, Taiyuan University of Science and Technology, Taiyuan 030024, People's Republic of China

processes of aged wood in historic buildings have been scarcely investigated so far. The decay of aged wood, manifesting as irreversible damage in the physical and mechanical properties, stems from changes in the microstructure of cell walls and the chemical components of wood. Therefore, identifying the deterioration mechanism of chemical components in wood is useful in selecting the appropriate remediation methods for historic wooden buildings.

Many world-renowned historic wooden buildings are in a warm, sunlit natural environment, such as the Imperial Palace in Beijing, China, Todaiji Buddha Temple in Nara, Japan, and Sungnyemun in Seoul, South Korea. These historic building are more susceptible to the influence of natural weathering, such as sunlight, oxygen, radiation, etc. Stalker [6] pointed that the most serious threat to wood indoors comes from thermal energy, and outdoors, from the combination of chemical, mechanical, and light energies. It is estimated that during the weathering process of over a few hundred years, the 10-mm-thick cladding (siding) on stave churches from Norway have been reduced by half [7]. As Wiesner [8] reported, weathering caused loss of the intercellular substance of wood and occurred the chemical changes. In the 1300-year-old wood taken from the Japanese wooden building under atmospheric conditions, microorganisms were found to be excluded but deterioration was still evident [9]. In the 20 years white pine wood under weathered outdoors, deterioration was also found, but cellulose appeared to be considerably less affected [10]. In other ancient wood samples from Japanese temple, the contents of hemicellulose and holocellulose decreased, but the crystallinity remained constant or slightly higher [11, 12]. Similar conclusions were reached for several 700–2700 years old oaks [13]. Also, lignin increased in fir wood from old buildings in Rychvald Castle, Czech Republic due to ageing [14]. Compared to normally non-exposed fresh wood, lignin was observed decreased in various kinds of wood exposed on a test fence for 30 years, and discoloration occurred under exposure in sunny, warm climates [15]. From these research works, it is known that natural weathering factors should be considered when discussing the conservation of ancient wood buildings. Further, in order to investigate the mechanism of natural weathering on wood, some scholars studied different artificial aging methods. Rapp et al using different bands of ultraviolet (UV) and visible (VIS) light found that photodegradation caused color changes in 288 samples of *Acer pseudoplatanus*, *Quercus robur*, *Picea abies* and *Juglans nigra* [16]. The paulownia wood was exposed to two test conditions: light under indoor conditions, and UV-induced ageing, highlighted that UV light from natural or artificial sources caused primarily lignin degradation [17]. Niemz et al. used an autoclave in N_2 atmosphere to accelerate wood aging and reported the degradation of hemicelluloses due to the heat treatment [18]. Lignin degradation after weathering was demonstrated by analyzing aspen wood samples exposed to accelerated weathering. The effects of weathering resulted in the wood surface lost their strength and the degraded parts were washed away by rainwater [15], which caused a reduction of the effective cross-section of components. The load-bearing cross-section of *Dou-Gong* brackets, the end of the beams and other structural nodes is very small, and the reduction of the effective cross-section due to deterioration is proportionally large compared to the original load-bearing cross-sectional area, which greatly reduces its load-bearing function and overall structural stability. However, as Blanchette et al. mentioned, the in-depth knowledge of these processes of aged wood is meager because such degradation to become obvious need extremely long time and the mechanism of wood degradation due to natural weathering is still obscure [19].

For the research on the material properties of historical wood structures, macroscopic observation, physical and mechanical performance testing are mostly used, such as density, moisture content, strength, elasticity, etc. However, some chemical changes occur in the chemical components of wood due to environmental factors. In this regard, some modern chemical characterization tools such as attenuated total reflectance fourier transform infrared (ATR FT-IR) spectroscopy and X-ray photoelectron spectroscopy (XPS) are particularly sensitive to the chemical state on the material surface, bringing irreplaceable results to this kind of research. ATR-FTIR was successfully employed to detect changing concentration of chromophoric groups on wood surfaces [20]. XPS, on the other hand, is particularly well suited for the study of surface chemistry of complex organic materials, by accurately providing information on the chemical bonds and charge distribution [21]. Despite their accuracy, the traditional methods require a larger number of materials for testing and long experiment period. The modern chemical characterization techniques, in comparison, require only a little amount of sample and no special preparation steps, while the results are highly sensitive, reliable, and accurate. They have allowed the less-destructive measurement of materials without changing its chemical and physical properties, can be used repeatedly on the same sample before more destructive analytical steps. These multiple chemical characterization techniques have a special place for the protection of cultural relics [22].

In this work, several samples of aged wood were taken from Yingxian Wooden Pagoda, China and used for multianalytical characterization. Scanning electron microscopy (SEM) was used to observe the morphology

of wood cell walls, and elemental analysis (EA) was applied to determine the main elemental contents. In addition, changes in the chemical components of the aged wood were qualitatively and quantitatively determined by ATR FT-IR spectroscopy and XPS techniques. This is the first interdisciplinary study for revealing the material deterioration mechanism in the Yingxian Wooden Pagoda; the obtained data may be useful for future conservation and restoration treatments, such as establishing a relationship between the surface photodegradation and strength loss and finding the appropriate protective coating and testing its weather resistance. This study also provides a theoretical basis for other research of Yingxian Wooden Pagoda and the diagnosis of similar historic wooden or masonry buildings.

Background

The Yingxian Wooden Pagoda is located in Yingxian County in the north of Shanxi Province, China (Fig. 1). Shanxi Province is in the middle of China by mountains. Due to its special geographical location, many historical architectures are scattered throughout the province (Fig. 1). Yingxian Wooden Pagoda is the oldest and tallest pagoda among the ancient wooden structures in China. It was erected in 1056 A.D. (Liao Dynasty). As a multi-story all-wooden structure without the use of nails, its grandiose scale and delicate details make it not only a major gem of ancient Chinese architecture but also a wonder in the history of world architecture.

The location of the pagoda has a temperate continental climate and is in a semi-arid region with plenty of sunshine and less rainfall. The annual evaporation is 4–5 times of the rainfall, which keeps the wood components dry. The prevailing wind direction in Ying County is southwest all the year round, and at a height of 49.8 m, the maximum wind speed is westerly, and the average wind speed is close to 15 m/s. Despite the ravages of nature, war, seismic disasters and so on during its lifetime, the main structure of the pagoda remains intact. However, properties of wood are bound to change as time goes on. In the surface of components like column and beam, original surfaces became rough, and the checks grow into large cracks (Fig. 2a, b). The Columns exposed to outdoor turned from the original wood color to a yellowing or browning that proceeds to an eventual graying, which gathered dirt and became unsightly (Fig. 2c). Other changes may also occur. The wood lost its surface coherence and became friable (Fig. 2d, e). Those fragments were easily broken off the surface and washed out by rainwater further erosion takes place, caused a reduction in the effective section of wooden components, as Fig. 2f–h shown in.

Fig. 1 Location of Yingxian Wooden Pagoda in Shanxi Province, China

In particular, the load-bearing cross-section of each *Dou-Gong* brackets (interlocking brackets characteristic of traditional Chinese buildings) is relatively small, and the reduction of the effective cross-section due to deterioration was proportionally large compared to the original load-bearing cross-sectional area, which greatly reduced its load-bearing function, resulting in other damage types such as splitting, crushing, and fracture generally existing in the pagoda. Similar features were also reflected in beams and columns. Damages such as tearing of the end of the beam and splitting of the column led to an increase in the contact surface area between the damaged components and the atmosphere, which in turn expanded the deterioration area and caused aggravated damage.

Materials and methods

Samples

To protect the pagoda and avoid secondary destruction of cultural relics, aged wood samples were carefully

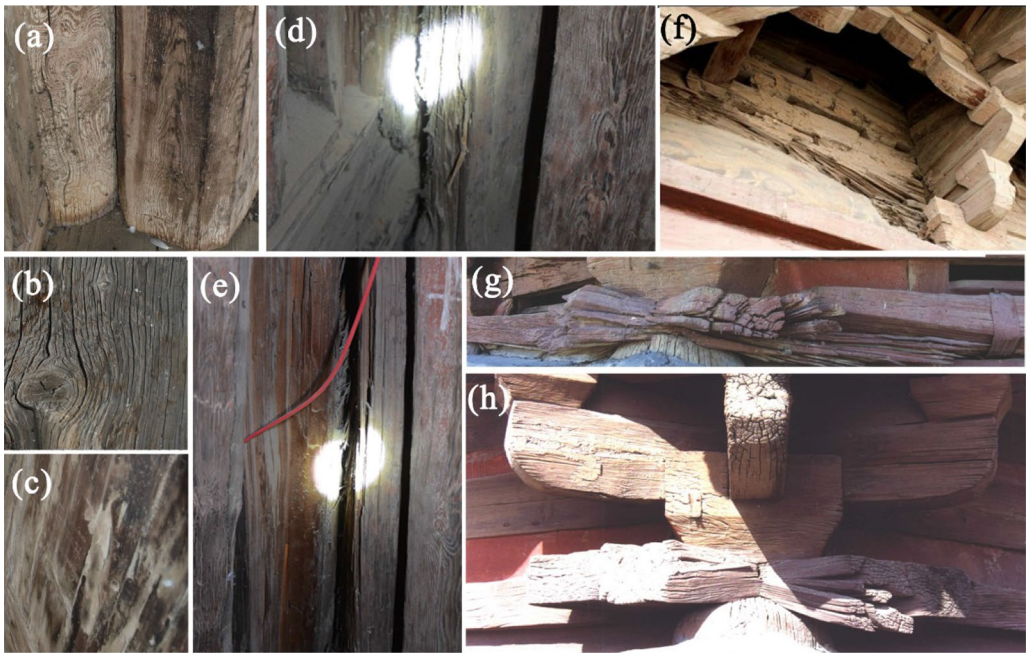

Fig. 2 **a–h** Deterioration of the wood components in Yingxian Wooden Pagoda

selected either as (1) broken fragments or (2) from concealed positions. A total of eight samples were collected using a surgical blade from the surface of columns or beam on each of the pagoda's nine floors (except the first floor), which were sampled from indoor and outdoor samples and were labeled F-1–F-8. There sampling positions, states of preservation, orientation and their descriptions are given in Table 1. Since no major weight-bearing components have been changed throughout the pagoda's history, these samples should come from the original parts. A previous study identified those samples as larch (*Larix principis-rupprechtii* Mayr.) [23], a tree species often used in historical buildings in North China. Therefore, contemporary and sound wood samples of the same species were used as references and named F-0. Samples were transported to the laboratory and stored in the dark and room temperature in a vacuum dryer to prevent moisture absorption before analysis.

Each sample was divided into two halves: one for XPS and EA analyses, and the other for the SEM and ATR FT-IR analyses. For the first half, a small amount of sample was cut into powder using surgical scissors and continually dried at room temperature. The other half was cut into thin, smooth wafers using a razor blade.

Characterization

Micro-morphology of the samples was inferred from SEM analysis through a JSM-6490LV instrument (JEOL,

Table 1 Description of the aged and reference wood samples

Sample	Material type	Provenance	Orientation	Macroscopic description
F-8-aged	Surface of external column	On the 9th floor	Northwest	Unwound, fragile
F-7-aged	Surface of internal column	On the 8th floor	West	Unwound, fragile
F-6-aged	Surface of external column	On the 7th floor	Southwest	Unwound, fragile
F-5-aged	Internal column, depth around 2 mm	On the 6th floor	Northeast	Hard, compact
F-4-aged	Surface of external column	On the 5th floor	North	Pulpy, shapeless
F-3-aged	Surface of internal column	On the 4th floor	North	Hard, compact
F-2-aged	Surface of external column	On the 3rd floor	North	Hard, compact
F-1-aged	Surface of internal beam	On the 2nd floor	Southwest	Hard, compact
F-0-sound	Wooden Pile	*Larix principis-rupprechtii* Mayr	–	Excellent

Japan). Samples were cleaned in demineralized water and manually cut along the using a razor blade. Then, they were mounted on the sample platform, covered by the conducting tape, and treated by the critical point dryer (JEOL, JFD-320). Finally, they were coated with a gold film (15 nm) in vacuum for 90 s (JEOL, JFD-1600). The SEM observation was conducted using an accelerating voltage of 20 kV, and the current of the electron beam was 300 mA. The magnifications were from × 50 to × 1000: the low one was used to observe the whole wood tissue, while the high magnification was used to study traces of sample decay. The preservation state of the aged wood samples was graded using the microscopically observed decays according to a new classification reported by Macchioni et al. [24].

The main elemental compositions of the samples were identified using EA (vario EL cube, Germany). A given amount (about 1.5 mg) of the sample was inserted into the combustion reaction tube within a tin or silver capsule. The measuring conditions were as follows. Carrier gas: pure oxygen, standard sample: sulfanilamide (CHNS mode), furnace temperatures: 1150 °C (comb. tube) and 850 °C (reduct. tube). The elements were identified using a thermal conductivity detector (TCD) by the produced gas (CO_2, SO_2, H_2O), which were separated by chromatographic column. Quantification was based on the peak area of each element, and the data were calibrated using standard test values as correction factors. Besides, the oxygen content was measured by the oxygen mode using an additional sample of about 2 mg. The carbon in the sample was converted into CO in pyrolysis and detected by TCD in the standard configuration. The standard sample was benzoic acid, and the furnace temperatures were 1150 °C (comb. tube) and 0 °C (reduct. tube).

ATR FT-IR characterization was performed on a Nicolet iS50 FT-IR spectrometer (Thermo Fisher Scientific Co., Waltham, MA, USA) equipped with a single-bounce diamond attenuated total reflection (ATR) device. The smooth side of the wood wafer was pressed against the ATR crystal by using a built-in pressure applicator. The FT-IR spectrum was recorded with a resolution of 4 cm^{-1} in the range between 400 and 4000 cm^{-1}. Each spectrum was obtained as the average of 32 successive scans in the absorbance mode. The spectral pre-processing of the wood samples used OMNIC™ software (Thermo Electron Corporation, Madison, WI, USA), including derivatives and smoothing in order to reduce noise. The data analyses were carried out employing Fourier self-deconvolution and Gaussian curve-fitting techniques using Origin software.

XPS spectra were recorded using a Kratos Axis Ultra spectrometer (Kratos Analytical Ltd., UK) with a hemispherical energy analyzer to investigate the chemical state of the samples, employing a monochromatic Al Kα X-ray source with a resolving power of 300 W. The powder sample was pre-evacuated overnight under a high vacuum of 10–9 mbar at room temperature. The spectrum was recorded for a typical surface area of 1 mm^2 and a depth less than 10 nm. The pass energy and resolution of the survey spectra were 160 eV and 1.0 eV/step in the lens in hybrid mode. Besides, the high-resolution spectrum of C 1*s* was acquired at a pass energy of 20 eV and resolution of 0.05 eV/step. The energy scale was calibrated using the aliphatic CC-carbon component at 285 eV. The background subtraction, deconvolution, and fitting of the C 1*s* spectra were performed using XPS PEAK 4.1 software.

Results and discussion

SEM

SEM observations were used to investigate the micromorphology of all samples along the tangential direction (Fig. 3) to identify the degree of degradation in the wood cell walls. Under microscopic magnifications, the sound reference sample showed well-preserved cell wall without damage. Meanwhile, the extent of decay varied greatly among the aged samples. Therefore, based on both the observations and the relevant literatures [24], those samples were classified into five categories of preservation (Table 2).

As shown in Table 2, apart from the sound wood (class I, Fig. 3a) that appeared unaffected, all eight aged wood samples were classified into four categories based on the extent of degradation on the examined sections. Among them, one sample was graded as II (F-1; Fig. 3b), two as III (F-2, F-5; Fig. 3c, d), four as IV (F-3, F-4, F-6, F-7; Fig. 3e–h), and one as V (F-8; Fig. 3i). Most of aged wood samples were in classes III or V, indicating a general trend of significant decay. Some samples showed only moderate signs of degradation (Fig. 3c); while in other cases the collapse, detachment, and distortions of cell walls were ubiquitous (Fig. 3f, g, h). The most decayed sample was F-8 (Fig. 3i), in which all cell walls completely collapsed, and the residue formed a mass without fixed form, leading to difficulties in identifying its morphology. Under SEM observation, Fig. 3 shows the degradation of bordered pits to varying degrees. For sample F-2 (class II, Fig. 3e), the pit openings were eroded and enlarged. Samples F-3 and F-6, classified as III, highlighted that the cracks have arisen through the pit, have a diagonal orientation, and expand to the cell wall around the pit (Fig. 3f, h). This type of cracks was observed by other authors [15, 25] when investigating the micro-crack formation of wood after exposure to sunlight for a period.

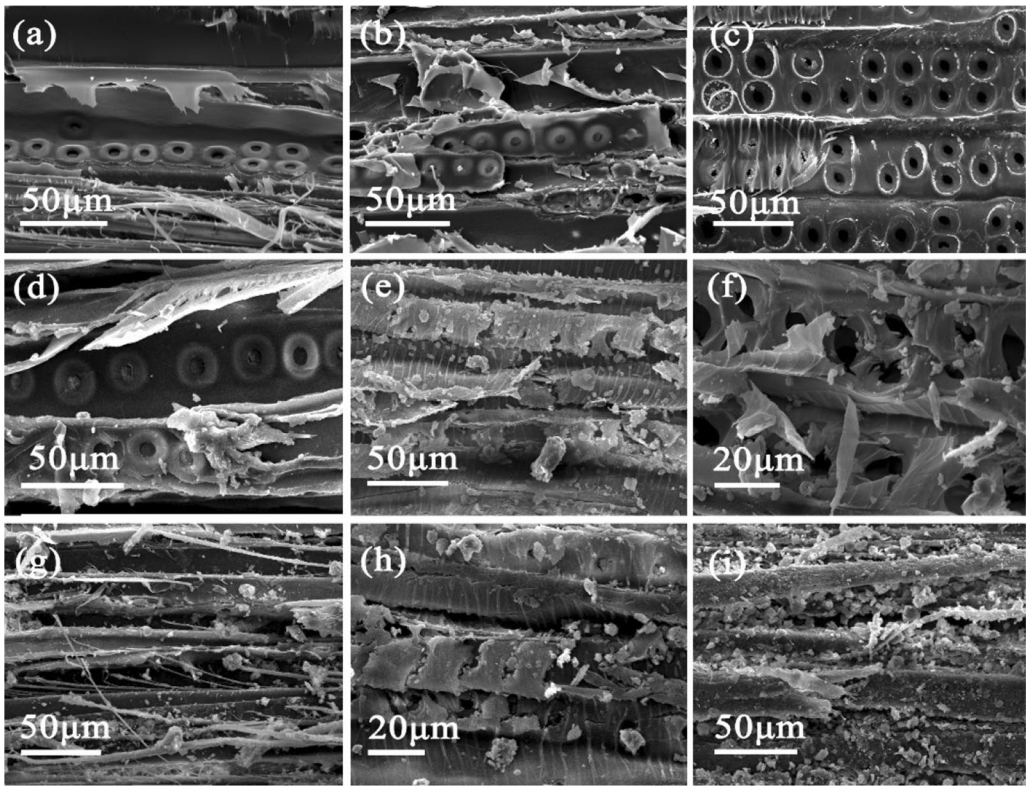

Fig. 3 The damage level of aged wood samples from SEM microanalysis. **a** F-0, class I; **b** F-1, class II; **c** F-2, class III; **d** F-5, class III; **e** F-3, class IV; **f** F-4, class IV; **g** F-6, class IV; **h** F-7, class IV; and **i** F-8, class V

Table 2 Classification of decay in the aged wood samples and sound sample

Damage level	Classification criteria	Samples
I	No sign of degradation. All cell walls are smooth and intact	F-0
II	Sporadic signs of degradation. Ray and tracheid cell walls well-preserved and almost intact. Only smaller cracks exist on a few cell walls	F-1
III	Some border pits, vessel, and ray cell walls are cracked and squeezed, showing moderate degradation of secondary walls	F-2, F-5
IV	Majority of cell walls are distorted, and the lumen often disappears. Some cells are more or less cracked along the micro-fibril angle, transforming the wall itself to strips of fibers	F-3, F-4, F-6, F-7
V	The cell walls have completely disintegrated, showing evident and widespread decay. Cell walls are extremely distorted, leading to the collapses of all cells. The identification of morphology can be very difficult	F-8

EA

The EA results of all investigated samples are summarized in Fig. 4a. Compared to the sound sample, most aged samples showed significant decline in the carbon content, while the variation of their oxygen content was slight. Since carbon and oxygen are the main elements of wood, the loss of carbon is probably ascribable to the degradation of low-molecular-weight or carbon-rich compounds such as fatty acids and terpenes, and the partial removal of lignin [21, 26, 27].

Due to the variation in the carbon and oxygen contents, the degradation degree may be more reliably assessed using the oxygen/carbon ratio (O/C). In the sound wood sample, O/C = 0.96, while the aged wood samples showed highly variable ratios in the range from 0.93 to 1.62 (Fig. 4b), and most of them are higher than those in the sound sample. According to the micro-morphological observation, the sample F-8 was classified at the least preserved (class V), and it also showed the highest O/C value (increased 68% from the reference). For the

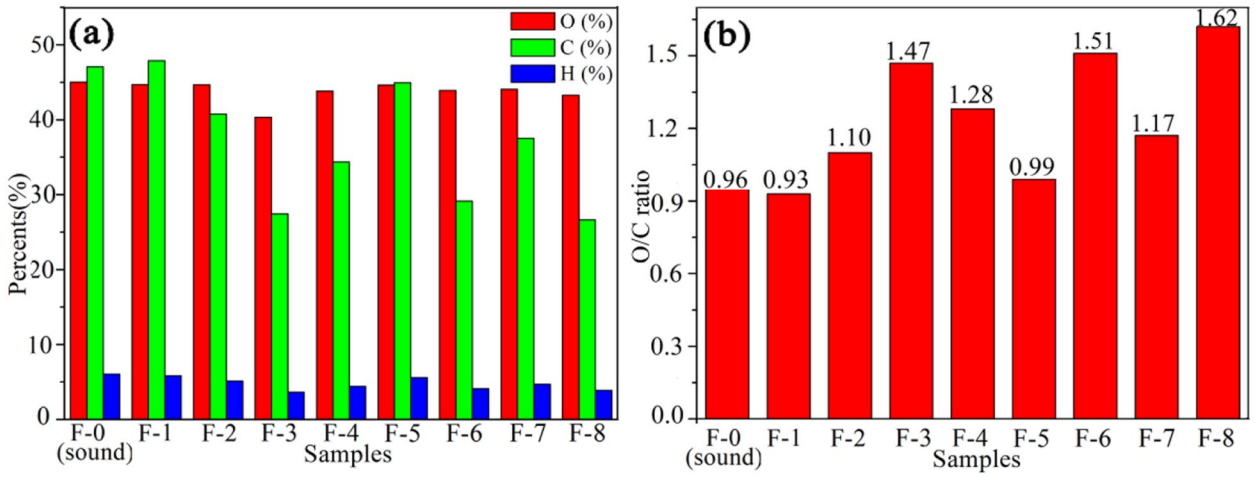

Fig. 4 **a** Elemental contents of the aged wood samples and the sound sample. **b** The O/C ratio of the aged and sound wood samples from EA

four samples in class IV, the O/C ratios were 1.17, 1.51, 1.28, and 1.47 for F-7, F-6, F-4, and F-3, respectively. On the contrary, samples classified as III and II (F-5, F-2, and F-1) showed no change or only a slight increase in the O/C ratio. Hence, the EA data were consistent with the results of micro-morphological classifications. In fact, the high O/C values of the aged wood indicate the possible chemical processes taking place in wood components.

ATR FT-IR

The ATR FT-IR spectra were obtained to better elucidate changes in the structure of wood constituents as well as their molecular functional groups. Figure 5 shows the survey spectra for all wood samples. The specific bands in the 1800–600 cm^{-1} fingerprint area were assigned to the main wood components (cellulose, hemicelluloses, and lignin). From the previous literature [28], all the bands can be easily assigned as summarized in Table 3. As expected, the spectra of sound wood sample contained almost all the peaks characteristic of lignin and cellulose, hemicelluloses.

The spectra of F-1, F-2 and F-5 seem to show similar bands with the sound wood sample, as seen in Fig. 5a, indicating their good preservation. However, when comparing the spectra for samples F-4, F-7and F-0 (Fig. 5b), the peaks of lignin (1596, 1508, 1451, 1422, 1333, and 1262 cm^{-1}) were present but their intensities were generally lower than those of polysaccharides at 1315 cm^{-1} and of water at 1635 cm^{-1}. Such difference appears to be attributable to the destruction of lignin to a certain extent. Notably, the largest spectral changes were seen in samples F-8, F-6, and F-3 (Fig. 5c, d). These spectra are dominated by the cellulose bands at 1030, 1103, 1315, 1370, and 896 cm^{-1}, while no peaks of lignin (1596, 1508, 1451, 1422, 1333, and 1262 cm^{-1}) were visible, indicating the depletion of lignin. The loss of lignin content was also observed in wooden components from several other historic buildings [14]. Besides, a new peak at 1616 cm^{-1} belonging to tannins appeared in samples F-6 and F-3 (Fig. 5d), further manifesting the molecular rearrangements and depolymerization of lignin. In coniferous wood, degraded lignin has a tendency towards condensation reactions [30]. As shown in Fig. 5, sound wood has an absorption peak at 1736 cm $^{-1}$, which is the stretching vibration absorption peak of acetyl group ($CH_3C=O$) in methanoglucuronic acid, and the disappearance of this characteristic peak in all aged wood samples indicates the degradation of its hemicellulose. The cellulose characteristic peaks at 1030, 1050, 1315, and 1370 cm^{-1} were the dominant peaks in the spectrum of the aged wood samples, demonstrating that the aged wood still contained a large amount of cellulose. Based on previous studies, the hemicellulose content of ancient wood was significantly decreased compared to sound wood, and the amorphous region of cellulose was partially degraded, which was due to the hydrolysis reaction of holocellulose caused by acid rain [31].

XPS

In the above, the significant reduction of carbon content have been discussed by EA analysis, and the decays of lignin and hemicelluloses in some aged wood samples detected by ATR FT-IR. Next, high-resolution scans of the XPS spectra of C 1*s* are used to obtain information concerning the chemical environment and structural alterations in the samples. From Fig. 6a–i, the C 1*s*

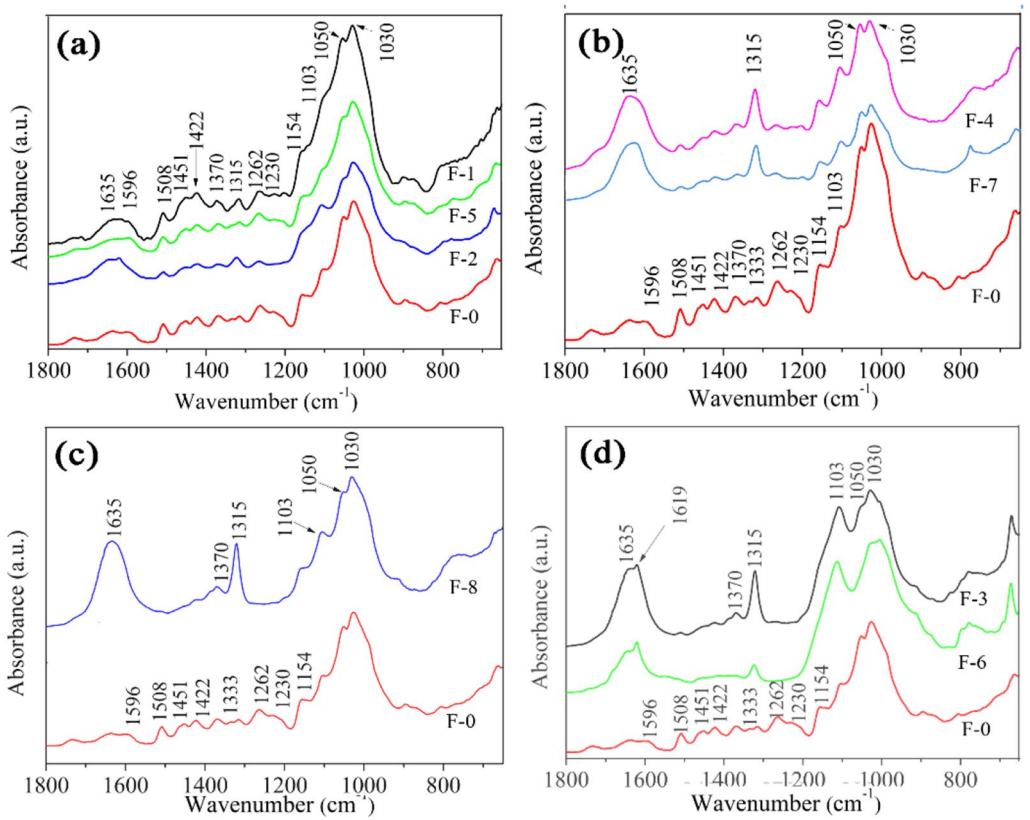

Fig. 5 **a–d** ATR FT-IR spectra of the sound sample and aged samples

Table 3 Assignment of infrared bands

Wave numbers (cm^{-1})	Functional group	Corresponding component
1736-1724	ν (C=O)	Cellulose, hemicelluloses
1660-1600	δ (H–O–H)	Water
1603-1594, 1510-1501	δ (C=C)	Lignin, aromatic skeleton
1456-1450, 1424-1417	δ (C–H)	Lignin
1370-1363	δ (C–H)	Cellulose, hemicelluloses
1352-1330	γ (CH_2), δ (O–H)	Lignin
1318-1309	ν (C–O–C)	Cellulose
1270-1266	ν (C=O)	Lignin, guaiacyl units
1234-1226	ν (C–O)	Cellulose, lignin
1156-1150	ν (C–O)	Lignin, xylan
1115-1092	ν (C–O–C)	Cellulose, hemicelluloses
1059-1050	ν (C–O)	Cellulose, hemicelluloses, lignin
1034-1024	ν (C–O)	Cellulose, hemicelluloses
895-900	δ (C–H)	Cellulose

spectrum of all samples share a wide peak for lignocellulosic materials, which is generally deconvoluted to obtain four types of carbon atoms.

The C_1 peak represents a carbon atom linked to other carbon atoms and/or hydrogen atoms (C–C, C–H), and this is related to lignin and wood extractives. The C_2 peak is identified as a carbon linked an oxygen atom by a single bond (C–O), assigned to cellulose. The C_3 peak is associated with a carbon bonded to two non-carbonyl oxygen atoms or in a carbonyl (C=O, O–C–O), which is mainly from functional groups of aldehydes, ketones, and acetals. Finally, the C_4 peak corresponds to a carbon atom bonded to a carbonyl and a non-carbonyl oxygen atom (i.e., a carboxylic group) [32].

Table 4 lists the binding energy and area under the decomposed C 1*s* peak for all investigated wood samples. Differences between the aged samples and sound sample can be seen in Fig. 6 and Table 4. In the aged samples, the area of C_1 peak was significantly smaller than that in the sound sample, while the area of C_2 peak increased. This may indicate that the cellulose did not undergo significant changes, but the extracts and lignin were degraded. These results are in good accordance to the variation observed in FT-IR spectra for the characteristic peaks of lignin and cellulose. In addition, there was a slight increase in the areas of C_3 and C_4 peaks, due to the raised content of organic acids, aldehydes,

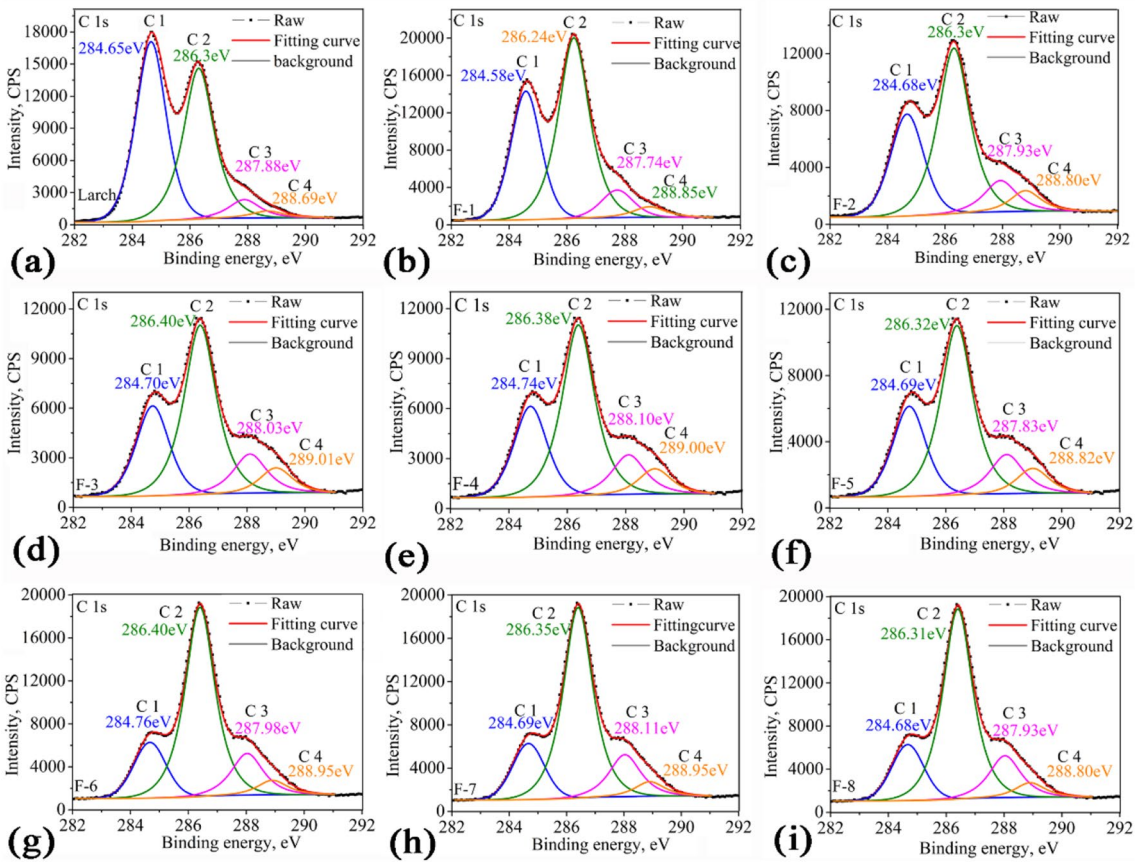

Fig. 6 XPS spectra of **a** the sound sample and **b–i** aged samples F-1–F-8, respectively

Table 4 XPS C 1*s* peaks of the sound and aged wood surfaces

	Carbon type	F-0 (sound)	F-1	F-2	F-3	F-4	F-5	F-6	F-7	F-8
Binding energy (eV)	C1	284.66	284.58	284.68	284.70	284.74	284.69	284.76	284.69	284.68
	C2	286.25	286.24	286.30	286.40	286.38	286.32	286.40	286.35	286.31
	C3	287.80	287.74	287.93	288.03	288.10	287.83	287.98	288.11	287.93
	C4	288.80	288.85	288.80	289.01	289.00	288.82	288.95	288.95	288.80
Area (%)	C1	47.78	34.87	31.67	23.16	27.10	25.79	21.39	21.31	21.27
	C2	44.33	54.36	52.18	58.51	52.72	61.24	56.92	47.68	56.34
	C3	5.53	7.43	9.65	11.53	12.37	8.28	17.14	23.46	14.95
	C4	2.37	3.34	6.50	6.80	7.81	4.69	4.54	7.55	7.43
	Ratio	1.09	1.87	2.16	3.32	2.69	2.88	3.68	3.69	3.70

*Ratio = C_{ox}/C_{unox}

* Cox/Cunox Ratio = oxygenated carbons/unoxygenated carbon= (C2+C3+C4) /C1

ketones, and acetals in the aged wood samples. The generation of conjugated carbonyls, carboxylic acids, and other products at the wood surfaces was due to the severe oxidation when the wood was exposed either outdoors or to artificial UV light [15, 33]. The ratio of C_{ox}/C_{unox} between oxygenated carbons ($C_2+C_3+C_4$) and unoxygenated carbon (C_1) was significantly higher in all aged samples than that in the sound wood sample (Table 4). In particular, the C_{ox}/C_{unox} ratios of sample F-8, F-6 and F-2 are higher than those of corresponding F-7, F-5 and F-1 respectively, which were consistent with the results of SEM and EA. The ratio of C_{ox}/C_{unox} can be attributed to the enhanced total amount of oxygen-carbon bonds, verifying the occurrence of

oxidation reactions on the surface of wood. Similar surface oxidation was observed by Popescu et al. in ageing-degraded lime wood (150–250 years) from panel paintings [21].

Deterioration mechanism

Combining the above results, the partial aged wood samples showed degradation of lignin. Normally, lignin is a very stable component in wood, exhibiting relatively strong resistance to hydrolysis due to its ether and carbon–carbon bonds. However, it is more sensitive to oxygen [34]. The aged wood samples in this study showed an enhanced total content of oxygen-carbon bonds, confirming the occurrence of oxidation reactions on their surface. A similar result was found by Hatakeyama et al., that a drop in wood lignin content can be induced by long-term oxidation processes [35]. Note that under ultraviolet radiation and air oxygen, the phenolic hydroxyl groups of lignin are prone to form phenoxyl radicals, which are the main intermediates of lignin degradation [36]. These phenoxyl radicals subsequently react with oxygen in degradation processes, as shown in Fig. 7. As a result, the macromolecular lignin depolymerizes to produce some chromophoric groups such as o-quinone and ρ-quinones, as well as some small soluble phenolic molecules like benzoic acid and benzaldehyde, eventually leading to a decrease in lignin content [36, 37]. Similar elevation in the contents of organic acids, aldehydes, and ketones was also detected in the present aged wood samples (Table 4). Comprehensive the results of these characterization, all aged wood samples had varying degrees of decay and lignin content was decreased in most of them. Actually, not only the wood collected from southwest, west, but also some wood samples collected from north, northwest and northeast were also partially affected by weathering, which indicating that the pagoda was affected by weathering in different directions.

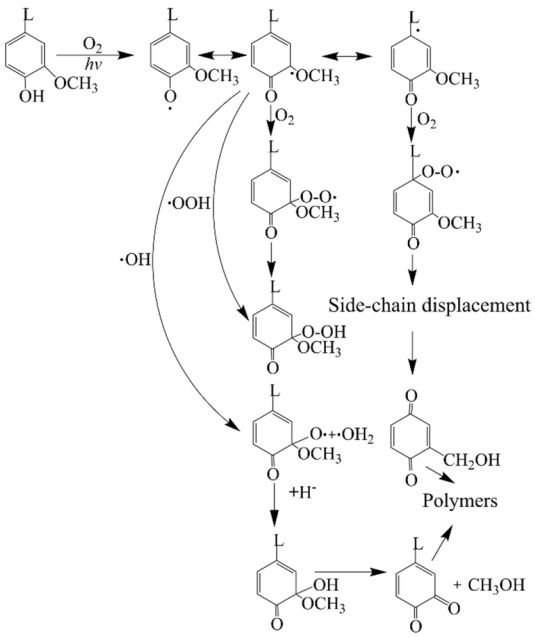

Fig. 7 Reaction of oxygen with lignin [36]

According to the literatures, archaeological waterlogged woods stored under wet dark and anaerobic conditions were mostly damaged by microorganisms [38]. This type of decay is mainly related to the depletion of polysaccharidic components, while lignin is relative stable component [39]. On the contrary, for historic wooden buildings in an aerobic and warm-dry environment, the wood deterioration mechanism is clearly different from most ancient wooden artifacts. Namely, there is a slow degradation of lignin, with the occurrence of oxidation reactions.

These degradation of the chemical components of cell walls would be reflected in the macroscopic properties. Several researchers have reported the weakened mechanical properties of wood after simulated photo-degradation, evidencing that sunlight exposure does reduce the strength of wood [40]. Derbyshire et al. reported a more than 80% reduction in the tensile strength of wood strips after 12 weeks of exposure to natural solar radiation [41]. Reliable and precise rates of photodegradation in wood were further proposed on this basis [42, 43]. Almeida et al. and Ouadou et al. showed that the loss in mechanical properties of wood due to natural weathering, including decreases in the strength and the modulus of elasticity and an increase in the elastic limit [44]. Another study emphasized the loss of tensile strength and the increase of cracks on wood surfaces due to weathering [45]. This continued degradation can affect the aging of wood surface. The surface may not be as dense as before and may be easily peeled off, which reduces an effective portion of the wooden components, thereby increasing the gap between the components. This seriously threatens the retention of the overall structure.

Conclusion

This study examined the wood decay process in Yingxian Wooden Pagoda, an 11th Century pagoda located in a warm-dry natural environment. Several aged wood samples were analyzed systematically by microscopic and chemical characterizations. Compared to the sound wood samples of the same tree species, all aged samples were found to have varying degrees of deterioration and some aged samples showed a reduction in lignin content, while those of cellulose remained constant or increased. In particularly, the increasing ratio of oxygenated carbon/

unoxygenated carbon demonstrated the occurrence of potential oxidation reactions.

Based on these results, we propose a wood deterioration mechanism that is slow degradation of lignin occurs due to oxidation reactions under the combination of sunlight, oxygen, and other environmental factors. These changes can result in the formation of macroscopic-to-microscopic intercellular and intracellular cracks or checks, which could decrease the strength of the aged wooden components. As weathering continues, rainwater washes out degraded portions of the wood and further erosion take place, which cause a reduction of the effective cross-section of components, and further greatly reduces its load-bearing function and overall structural stability.

Yingxian Wooden Pagoda is a large and complex structure with varying degrees and types of damaged wooden components. The diagnosis of the wood in such buildings, without causing any damage to them, is an urgent issue that needs to be addressed. This paper presents a multi-chemical analysis method to identify key factors in wood degradation. This method seems to be less invasive, with the advantages of limited sample amount, no required special preparation steps, and reusable on the same sample. These methods and results will also be useful for studying other historical wooden buildings under warm-dry conditions. In future, the relation of surface-degradation and structural weakening should be ascertained. Although some results have been reported on the photodegradation of wood, historic wooden buildings require the use of transplantation analysis of the results. By measuring the type and degree of wood strength loss and the depth, rate, and other parameters of photodegradation, it is possible to establish a relationship for assessing the need for protective measures in historic wooden buildings, and this should be a starting point for further investigation.

Based on the photodegradation revealed here, some harmless and colorless coating materials should be sought out, which can form a protective layer on the surface of aged wood to counteract the continuous surface deterioration. The main function of these coating materials is to protect the wood surface from the weathering elements (sun and water) and to help maintain its appearance. There are two basic types of finishes (or treatments) in existing materials used to protect wood surfaces: (1) finishes that form a film, layer, or coating on the wood surface (film-forming), and (2) finishes that penetrate the wood surface and leave no visible layer or coating (non-film-forming) [15]. Painted materials can offer the greatest protection because they are generally opaque to the degrading effects of UV light and protect the wood from moisture at various levels [46]. Surface treatments, such as water-repellent preservatives and certain inorganic chemicals (chromium compounds), enhance the transparency of the material to reflect the texture and inherent beauty of wood while significantly improving the properties of the wood [47]. Many aspects of wood weathering are not yet fully understood. A comprehensive understanding of the mechanisms involved in weathering will allow the development of new treatments and finishes, which will greatly enhance the durability of wood and provide greater protection against degradation.

Acknowledgements
We wish to thank the help of Shanxi Cultural Relic Bureau and Yingxian Cultural Relic Protection Department.

Author contributions
Conceptualization, MXC; experiment, MXC, LYQ; software, LJ; writing—original draft preparation, MXC and QXC; writing-review and editing, MXC, LYQ, QXC and LJ. All authors have read and agreed to the published version of the manuscript. All authors read and approved the final manuscript.

Funding
This study was supported by the National Natural Science Foundation of China (No. 51338001), Fundamental Research Program of Shanxi Province (No. 202103021223278), Teaching Reform and Innovation Project of Taiyuan University of Science and Technology (No. JG2022064), Taiyuan University of Science and Technology doctoral research start-up project (No. 20212068), Introducing Outstanding Doctoral Research Funding from Shanxi Province (No. 20222141).

Availability of data and materials
Most of the data on which the conclusions of the manuscript rely is published in this paper, and the full data is available for consultation on request.

Declarations

Competing interests
We declare that there is no actual or potential conflict of interest, financial or otherwise, within 3 years from the beginning of the submitted work, that could inappropriately influence or be perceived as influencing an author's objectivity.

Received: 29 January 2023 Accepted: 9 May 2023
Published online: 18 May 2023

References

1. Meng XJ, Li TY, Yang QS. Experimental study on the seismic mechanism of a full-scale traditional Chinese timber structure. Eng Struct. 2019;180:484–93.
2. Gao C, Wang J, Yang QS, et al. Analysis of rocking behavior of tang-song timber frames under PULSE-type excitations. Int J Struct Stab Dyn. 2019;20(8):1–33.
3. Han JL, Qiao GF, Niu QF, et al. Finite element analysis of typical beam–column joints in yingxian wood pagoda. Adv Mater Res. 2014;1008–1009:1205–8.
4. Chen Z, Zhu E, Lam F, et al. Structural performance of Dou-Gong brackets of Yingxian Wood Pagoda under vertical load—an experimental study. Eng Struct. 2014;80:274–88.
5. Xu L, Li TY. Material properties test of wooden architecture and its mechanical properties. Advanced Materials Research. 2013;788(788):651–5.
6. Stalker IN. Protection of timber from fire and weathering. Chem Ind Lond. 1971;35(50):1.

7. Borgin K, Faix O, Schweers W. The effect of aging on lignins of wood. Wood Sci Technol. 1975;9:207–11.
8. Wiesner J. Untersuchungen über die herbstliche Entlaubung der Holzgewächse. Sitzungsber Akad Wiss Wien. 1871;64:465–510.
9. Yonenobu H, Tsuchikawa S. Near-infrared spectroscopic comparison of antique and modern wood. Appl Spectrosc. 2003;57(11):1451–3.
10. Browne FL. Unpublished Report; U.S. Department of Agriculture, Forest Service, Forest Products Laboratory: Madison, WI; 1957.
11. Tsuchikawa S, Yonenobu H, Siesler HW. Near-infrared spectroscopic observation of the ageing process in archaeological wood using a deuterium exchange method. Analyst. 2005;130(3):379–84.
12. Saito YS, Shida M, Ohta H, et al. Deterioration character of aged timbers: insect damage and material aging of rafters in a historic building of Fukushoji-temple. Mokuzai Gakkaishi. 2008;54:255–62.
13. Sandak A, Sandak J, Zborowska M, et al. Near infrared spectroscopy as a tool for archaeological wood characterization. J Archaeol Sci. 2010;9:0–2101.
14. Kačík FP, Šmíra P, Kačíko D, et al. Chemical changes in fir wood from old buildings due to ageing. Cellul Chem Technol. 2014;48(1–2):79–88.
15. Feist WC. Outdoor wood weathering and protection. American Chemical Society; 1989.
16. Rapp AO, Peters FB. Wavelength-dependent photodegradation of wood and its effects on fluorescence. Holzforschung. 2022;76(1):60–7.
17. Liu XY, Timar MC, Varodi AM, et al. Effects of ageing on the color and surface chemistry of paulownia wood (P. Elongata) from fast growing crops. Bioresources. 2016;1(4):9400–20.
18. Niemz P, Hofmann T, Rétfalvi T. Investigation of chemical changes in the structure of thermally modified wood. Maderas Ciencia Y Tecnología. 2010;12(2):69–78.
19. Blanchette RA, Haight JE., Koestler RJ., et al. Assessment of deterioration in archaeological wood from ancient Egypt. J Am Inst Conserv. 1994;33(1):55–70.
20. Pandey KK, Vuorinen T. Comparative study of photodegradation of wood by a UV laser and a xenon light source. Polymer Degrad Stab. 2008;93(12):2138–46.
21. Popescu CM, Tibirna CM, Vasile C. XPS characterization of naturally aged wood. Appl Surf Sci. 2009;256(5):1355–60.
22. Sandak A, Sandak J, Zborowska M, et al. Near infrared spectroscopy as a tool for archaeological wood characterization. J Archaeol Sci. 2010;37(9):0–2101.
23. Fan C, Wang L, Peng J. Measures to control seasoning checks of wood used for the repair of the ancient wooden tower in Yingxian County, Shanxi Province. J Beijing For Univ. 2006;28(1):98–102.
24. Macchioni N, Capretti C, Sozzi L, et al. Grading the decay of waterlogged archaeological wood according to anatomical characterisation. The case of the Fiavé site (N-E Italy). Int Biodeter Biodegrad. 2013;84(84):54–64.
25. Sandberg D, Söderström O. Crack formation due to weathering of radial and tangential sections of pine and spruce. Wood Mat Sci Eng. 2006;1(1):12–20.
26. Nzokou P, Kamdem DP. X-ray photoelectron spectroscopy study of red oak-(*Quercus rubra*), black cherry-(*Prunus serotina*) and red pine-(*Pinus resinosa*) extracted wood surfaces. Surf Interf Anal. 2005;37:689–94.
27. Popescu CM, Dobele G, Rossinskaja G, et al. Degradation of lime wood painting supports. Evaluation of changes in the structure of aged lime wood by different physico-chemical methods. J Anal Appl Pyrolysis. 2007;79:71–7.
28. Emandi A, Vasiliu CI, Budrugeac P, et al. Quantitative investigation of wood composition by integrated FT-IR and thermogravimetric methods. Cellul Chem Technol. 2011;45(9):579–84.
29. Guo J. Effects of ageing on the cell wall and its hygroscopicity of wood in ancient timber construction. Wood Sci Technol. 2018;52(1):1–17.
30. Colombini MP, Orlandi M, Modugno F, et al. Archaeological wood characterization by PY/GC/MS, GC/MS, NMR and GPC techniques. Microchem J. 2007;85(1):164–73.
31. Mi XC, Li TY, Wang JP, et al. Evaluation of salt-induced damage to aged wood of historical wooden buildings. Int J Anal Chem. 2020;1:1.
32. Inari GN, Petrissans M, Lambert J, et al. XPS characterization of wood chemical composition after heat-treatment. Surf Interface Anal. 2006;38(10):1336–42.
33. Hon NS, Feist WC. Weathering characteristics of hardwood surfaces. Wood Sci Technol. 1986;20(2):169–83.
34. Kránitz K, Sonderegger W, Bues CT, et al. Effects of aging on wood: a literature review. Wood Sci Technol. 2016;50(1):7–22.
35. Hatakeyama H, Hatakeyama T. Lignin structure, properties, and applications. Bull Am Phys Soc. 2009;2009:1–63.
36. Paulsson M, Parkås J. Review light induced yellowing of lignocellulosic pulps-Mechanisms and preventive method. BioResources. 2012;7(4):5995–6040.
37. Laura L, Teischinger A, Hansmann C, et al. Wood surface discolouration due to simulated indoor sunlight exposure. Holz als Roh- und Werkstoff. 2007;66(1):51–6.
38. Broda M, Popescu CM. The natural decay of archaeological oak wood versus artificial degradation processes—an FT-IR spectroscopy and X-ray diffraction study. Spectrochim Acta Part A Mol Biomol Spectrosc. 2018;209:280–7.
39. Sandak A, Sandak J, Riggio M. Assessment of wood structural members degradation by means of infrared spectroscopy: an overview. Struct Control Health Monit. 2016;23(3):396–408.
40. Altgen M, Militz H. Photodegradation of thermally-modified Scots pine and Norway spruce investigated on thin micro-veneers. Eur J Wood Wood Prod. 2016;74(2):185–90.
41. Derbyshire H, Miller ER, The photodegradation of wood during solar irradiation. Part 1. Effects on the structural integrity of thin wood strips. Holz Roh Werkstoff. 1981;39:341–50.
42. Derbyshire H, Miller ER, Turkulin H, Investigations into the photodegradation of wood using microtensile testing. Part 1: the application of microtensile testing to measurement of photodegradation rates. Holz Roh Werkstoff. 1995;53:339–45.
43. Derbyshire H, Miller E, Turkulin H, Investigations into the photodegradation of wood using microtensile testing. Part 2: an investigation of the changes in tensile strength of different softwood species during natural weathering. Holz Roh Werkstoff. 1996;54:1–6.
44. Ouadou Y, Aliouche D, Thevenon MF, et al. Characterization and photodegradation mechanism of three Algerian wood species. J Wood Sci. 2017;63(3):288–94.
45. Evans PD, Urban K, Chowdhury MJ. Surface checking of wood is increased by photodegradation caused by ultraviolet and visible light. Wood Sci Technol. 2008;42(3):251–65.
46. Feist WC. Finishing wood for exterior use. Proceedings 87318—finishing eastern hardwoods. 1983:185–98.
47. Black JM, Mraz EA. Inorganic surface treatments for weather-resistant natural finishes. Inorganic Surface Treatments for Weather-Resistant Natural Finishes; 1974.

Publisher's Note